ADVANCED FUNCTIONAL MATERIALS
www.afm-journal.de

Rapid and Controllable Multilayer Cell Sheet Assembly via Biodegradable Nanochannel Membranes

*Letao Yang, Christopher Rathnam, Yannan Hou, Misaal Patel, Li Cai, and Ki-Bum Lee**

The ability to precisely arrange and control the assembly of diverse cell types into intricate 3D structures remains a critical challenge in tissue engineering. Herein, a versatile and programmable 3D cell sheet assembly is described technology by developing a biodegradable nanochannel (BNC) membrane to fulfill this unmet need. This membrane, hierarchically assembled from 2D nanomaterial aggregates, exhibits both exceptional fluid permeability and rapid biodegradation under physiological conditions. The unique properties of the BNC membrane enable precise spatial and temporal control over cell assembly, facilitating the creation of complex 3D cellular architectures. The BNC membrane is integrated with a programmable negative-pressure-based cell assembly strategy to form single and multicellular 3D sheets in a highly controllable manner. To demonstrate the feasibility and translatability of this technology in the field of tissue engineering approaches to screen stem cell-derived therapeutics with "core–shell" macrophage-fibroblast multicellular patterns and treat murine diabetic skin wounds via scaffold-free 3D adipose-derived mesenchymal stem cell (ADMSC) sheets are devised. In summary, the results demonstrate that the BNC membrane-based 3D cell sheet assembly approach significantly advances current tissue engineering capabilities, offering substantial potential for both regenerative medicine applications and the development of physiologically relevant disease models.

1. Introduction

Precise control over cellular spatial arrangement is fundamental to successful tissue engineering, as it directly governs tissue function, construct efficacy and the faithful recapitulation of native tissue architecture. This level of control is essential for fostering appropriate cell–cell interactions and ultimately generating functional tissue replacements.[1] The development of advanced techniques for realizing controlled cell assembly has facilitated the creation of more representative in vitro disease models and the construction of functional tissue replacements for in vivo regenerative medicine.[2] To effectively model diseases, it is imperative to ensure the controllable assembly of cells into tissues.[3] Oversimplified tissue models may limit the translational potential of therapeutics tested on these disease models.[4] Similarly, current cell replacement therapies in regenerative medicine often fall short of optimal efficacy due to inadequate control over the spatial and temporal assembly of cells into functional tissues. This limitation hinders the formation of physiologically relevant structures and compromises therapeutic outcomes.[5] Although scaffold-based patterning techniques, such as soft lithography and photoresponsive hydrogels, offer varying degrees of control over cell assembly, it is necessary to independently investigate the individual effects of patterned cells and the surrounding material-mediated cues.[6] This becomes a barrier to achieving accurate understanding of tissue formation and developing optimal cell assembly strategies. While 3D bioprinting of scaffold-free spheroids offers a promising solution to this challenge,[7] the process of spheroid formation is typically slow, and the resolution of resulting cell patterns

L. Yang
Key Laboratory of Spine and Spinal Cord Injury Repair and Regeneration of Ministry of Education, Department of Orthopedics, Tongji Hospital affiliated to Tongji University, Frontier Science Center for Stem Cell Research, School of Life Science and Technology
Tongji University
Shanghai 200065, China

The ORCID identification number(s) for the author(s) of this article can be found under https://doi.org/10.1002/adfm.202403367

DOI: 10.1002/adfm.202403367

L. Yang, C. Rathnam, Y. Hou, K.-B. Lee
Department of Chemistry and Chemical Biology
Rutgers
The State University of New Jersey
Piscataway, NJ 08854, USA
E-mail: kblee@rutgers.edu

M. Patel, L. Cai, K.-B. Lee
Department of Biomedical Engineering
Rutgers
The State University of New Jersey
Piscataway, NJ 08854, USA

is often unsatisfactory, with precision limited to the scale of tens of microns.[8]

For this purpose, a plethora of methods have been developed to achieve high throughput and accurate cell assembly in a scaffold-free manner, including magnetic, electrical, or other physical field-guided approaches.[8] However, these approaches require additional steps of attachment and removal of magnetic nanoparticles or have to be performed in a buffer with low ionic forces that may compromise biocompatibility during assembly.[9] Another approach to achieving precise scaffold-free 3D cell assembly involves the functionalization of cell membranes with bio-recognition molecules, particularly complementary DNA ligands.[10] However, the extensive modifications of cell membranes with DNA may lead to genetic interferences in cells after assembly.[11] Cell sheet engineering approaches based on the thermoresponsive [e.g., Poly(N-isopropylacrylamide)] or other stimuli-responsive polymers have also been developed to address the aforementioned challenges in scaffold-free tissue engineering.[4] However, they typically form fragile single-layer cell assemblies that lack 3D cell-cell interactions. In addition, the multicellular patterning of diverse cell types, which is desirable for recapitulating complex tissues, is also challenging for current cell sheet engineering approaches. Given these limitations, there remains a critical need to develop innovative cell assembly strategies that can advance the field of tissue engineering and enable more sophisticated cellular constructs. Such novel approaches are essential for overcoming current barriers to creating complex, functional tissues for both research and clinical applications.

Chronic wounds that exhibit slow-healing properties can escalate into conditions that pose significant threats to life.[12,13] One promising treatment option for diabetic wounds (e.g., diabetic ulcers) has been the implementation of stem cell therapy. However, current stem cell implantation methods and evaluation models heavily rely on improvements in controlled cell assembly.[14,15] Therefore, developing efficient, accurate, and reliable techniques for controlling cell assembly could thus advance both stem cell transplantation outcomes and facilitate the screening of stem cell-derived therapeutics, thereby improving the treatment of chronic wounds.

Addressing the aforementioned challenges, we developed an innovative multilayer cell assembly technology that can: i) create single- and multicellular patterns in a precise manner; ii) form robust multilayered tissues rapidly at minute-scale; and iii) generate scaffold-free tissues after cell assembly. Remarkably, our cell assembly technique utilizes a biodegradable nanochannel (BNC) membrane, hierarchically assembled from 3D manganese dioxide (MnO_2) nanosheet aggregates, which exhibit excellent permeability and rapid biodegradability. In order to generate the cell patterns, a mask with pre-defined geometry is carefully positioned on the BNC membrane. When the BNC membrane is connected to negative pressure and single-cell suspensions are added to the mask, the cells spontaneously follow the shape of the negative pressure field. Due to the existence of negative pressure, diverse cell types, including the non-adherent cells (e.g., monocytes) could be rapidly assembled within a few minutes for versatile applications (**Figure 1a**). Additionally, the assembled cell sheets could also be controlled with their multilayered structure. Most importantly, by optimizing the BNC membrane structure to achieve fast biodegradation under physiological concentrations of Vitamin C, the multilayer cell sheets could be readily harvested in a scaffold-free manner (Figure 1b). To demonstrate the feasibility and translatability of this technology in the field of tissue engineering, we devised approaches to screen stem cell-derived therapeutics with "core–shell" macrophage-fibroblast multicellular patterns (Figure 1b) and treat murine diabetic skin wounds via scaffold-free 3D adipose-derived mesenchymal stem cell (ADMSC) sheets (Figure 1c). The significant improvement in the healing process and the overall histology of the wound strongly supports the therapeutic potential of 3D ADMSC sheets generated by the BNC-based method for treating diabetic wounds (Figure 1c,d). Thus, we successfully demonstrated the BNC membrane-based method as a promising means for rapid, accurate, and programmable 3D cell assembly applicable for both tissue engineering and disease modeling.

2. Results and Discussions

2.1. Fabrication of Biodegradable Nanochannel (BNC) Membrane

We first sought a method to develop a BNC membrane with the desired qualities of rapid and controllable biodegradability. Furthermore, we aimed to incorporate tunable nanochannels into the membrane, which would provide exceptional permeability for fluid flow and support the negative pressure-guided assembly. Different types of nanochannel membranes have been developed for filtration applications in varying biomedical and engineering applications.[16–18] For instance, polymeric membranes have been widely developed and utilized for various filtration applications in combination with the negative pressure field-guided particle assembly.[16] Nevertheless, the biodegradation process of these polymers primarily depends on pH-induced hydrolysis, which may not be suitable for all biological environments. Enzymatic degradation of biopolymers is less dependent on pH compared to other degradation methods. However, the degradation of these membranes becomes less efficient when degrading macroscopic membranes without using excessive enzymes, which is costly and limited in efficiency. This limitation arises because most enzymes are large molecules that do not diffuse as rapidly as small molecules, hindering their ability to degrade the material effectively.

To the best of our knowledge, there is a lack of membranes that can quickly degrade under biological conditions without compromising the viability of surrounding cells.[18,19] To address this challenge, we fabricated the BNC membrane through the vacuum filtration of 3D hierarchical MnO_2 nanostructures. We focused on MnO_2 nanomaterials as the membrane building blocks due to their fast biodegradation rates (1–3 orders of magnitude higher than existent polymeric materials), as reported by us and other groups recently.[20] To promote degradation under physiological conditions, we used a vacuum filtration-mediated bottom–up assembly approach to ensure a flat surface. Additionally, this provided a location to assemble cells in an organized manner.[21]

To investigate the structure-function relationship of the BNC membranes (**Figure 2a–c**; Figures S1, S2, Supporting Information), we created three different BNC membranes from MnO_2 nanoneedles (1D nanostructures), nanosheets (2D nanostructures), and nanosheet-stacked 3D nanostructures, named 1D-BNC, 2D-BNC, and 3D-BNC membrane, respectively. We

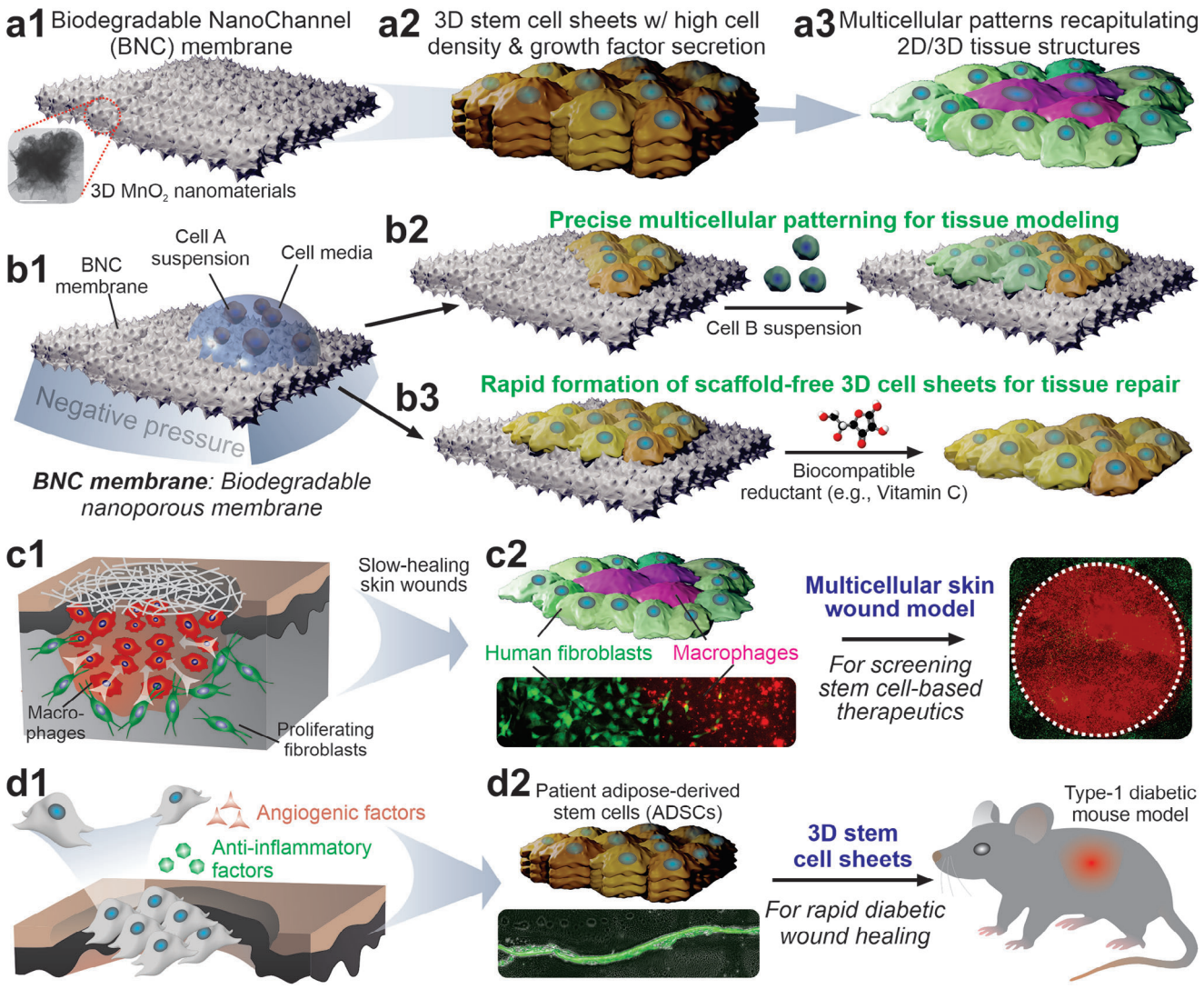

Figure 1. Enhanced stem cell-based skin wound treatment by developing a biodegradable nanochannel membrane-mediated cell assembly approach. a) Schematic diagrams illustrating our strategy of improving the treatment of slow-healing skin wounds by developing advanced wound models and enhanced stem cell therapies. Specifically, advanced wound models would require the recapitulation of multicellular tissue structures of human skins using human cells. Advancements in stem cell therapies would require a better enhancement of stem cell survival in vivo for sustained secretion of trophic factors. b) Our strategy of developing a biodegradable nanochannel (BNC) membrane-based cell assembly for scaffold-free stem cell transplantation and to create multicellular patterns for disease and tissue injury modeling. The BNC membrane is connected to and permeable to a negative pressure field, which guides the assembly of cells into designated areas on the BNC membrane by controlling the media flow. Following the cell assembly procedure makes it possible to extract a 3D stratified tissue without the need for scaffolding, making it suitable for transplantation. The complex multicellular patterns formed on the BNC membrane offer valuable resources for tissue modeling applications. c) Improved treatment of slow-healing wounds using our BNC membrane-based cell assembly method. The benefits of using our method are two-fold. First, the precision creation of a unique macrophage-fibroblast tissue pattern closely mimicking the inflammation stage of diabetic wound healing can allow more efficient screening of stem cell-based therapeutics. Second, as shown in the right panel, the formation of scaffold-free 3D stem cell sheets improved stem cell transplantation and therapeutic outcomes in vivo to accelerate wound healing in a murine diabetic wound model.

confirmed the superior performance of the 3D-BNC in terms of both rapid biodegradation (within 5 min) under biocompatible stimuli (e.g., 1 mg mL^{-1} Vitamin C) and excellent permeability to the underneath negative pressure fields (characterized by vacuum filtration rates of the membrane) (Figure 2d–f).[22] This is because 2D nanosheets during vacuum filtration tend to stack on top of the cellulose filter paper, preventing the formation of pores and the transport of biomolecules. In contrast, the isotropic geometry of 3D MnO_2 allows for the existence of void volume within the scaffold, effectively serving as nanochannels. When nanosheets were stacked parallel, the formed membranes would be densely packed and not permit the existence of any void volume, thereby preventing the formation of nanochannels. Although 1D MnO_2 nanoneedles were successfully assembled into the nanochannel membrane (confirmed by FESEM) with high permeability to negative pressure field, their biodegradation rates are 4–5 folds slower than the 3D-BNC, which substantially compromises the viability of cells during the retrieval of cell

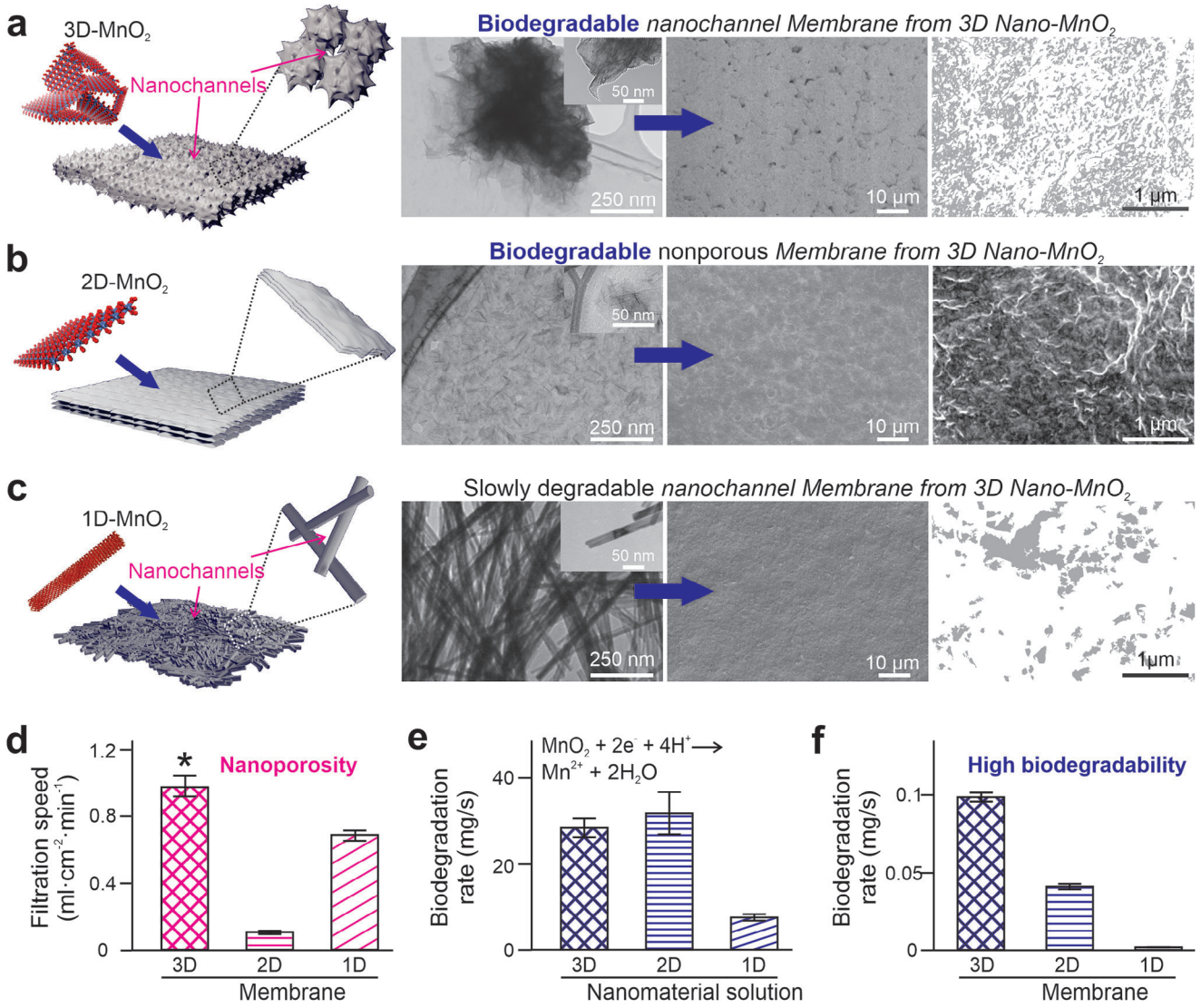

Figure 2. A biodegradable nanochannel (BNC) membrane assembled from 3D hierarchical MnO_2 nanostructures. a–c) Schematic diagram and electron microscope images showing the generation of 3D biodegradable membranes from 3D-, 2D-, and 1D-MnO_2 nanomaterials. d–f) Quantitative analysis of nanoporosity, in-solution biodegradability, and in-membrane biodegradability of BNC membranes assembled from 3D-, 2D-, and 1D- MnO_2 nanomaterials. $n = 3$ experimental replicates. $^*p < 0.05$ by one-way ANOVA with Tukey post-hoc analysis.

assemblies due to extended co-culture with Vitamin C. This observation is consistent with previous reports, as 1D nanoneedle crystals have a lower surface area than 2D nanosheets. Indeed, 2D MnO_2 nanosheets in their solution form showed similar biodegradation rates compared to 3D MnO_2 hierarchical nanomaterials but were much faster than the 1D MnO_2 nanoneedles (Figure 2f). However, once assembled in parallel on the 2D-BNC, the biodegradation rates became significantly slower, with a two-fold increase in complete degradation time compared to the 3D-BNC membrane. Moreover, the filtration speed through the 2D-BNC membrane under an identical negative pressure field is significantly impeded compared to both 1D-BNC and 3D-BNC membranes. This could be because the parallelly stacked nanosheets in the 2D-BNC membrane do not support pore formation (Figure 2a), reducing the surface area desired for degradation and decreasing the permeability to the underneath negative pressure field. Furthermore, we confirmed the biocompatibility of the 3D-BNC membrane in vitro using PrestoBlue cell viability assays. This innovative 3D-BNC membrane boasts a fast degradation rate, adjustable nanochannels, and excellent biocompatibility.

2.2. Rapid, Controllable, and Retrievable Cell Assembly on BNC Membrane

Next, we developed BNC membrane-based approaches for the controllable cell assembly and formation of scaffold-free 3D cell sheets (**Figure 3**). With the latest development in vacuum-based microfluidics featuring cell trapping capabilities and the

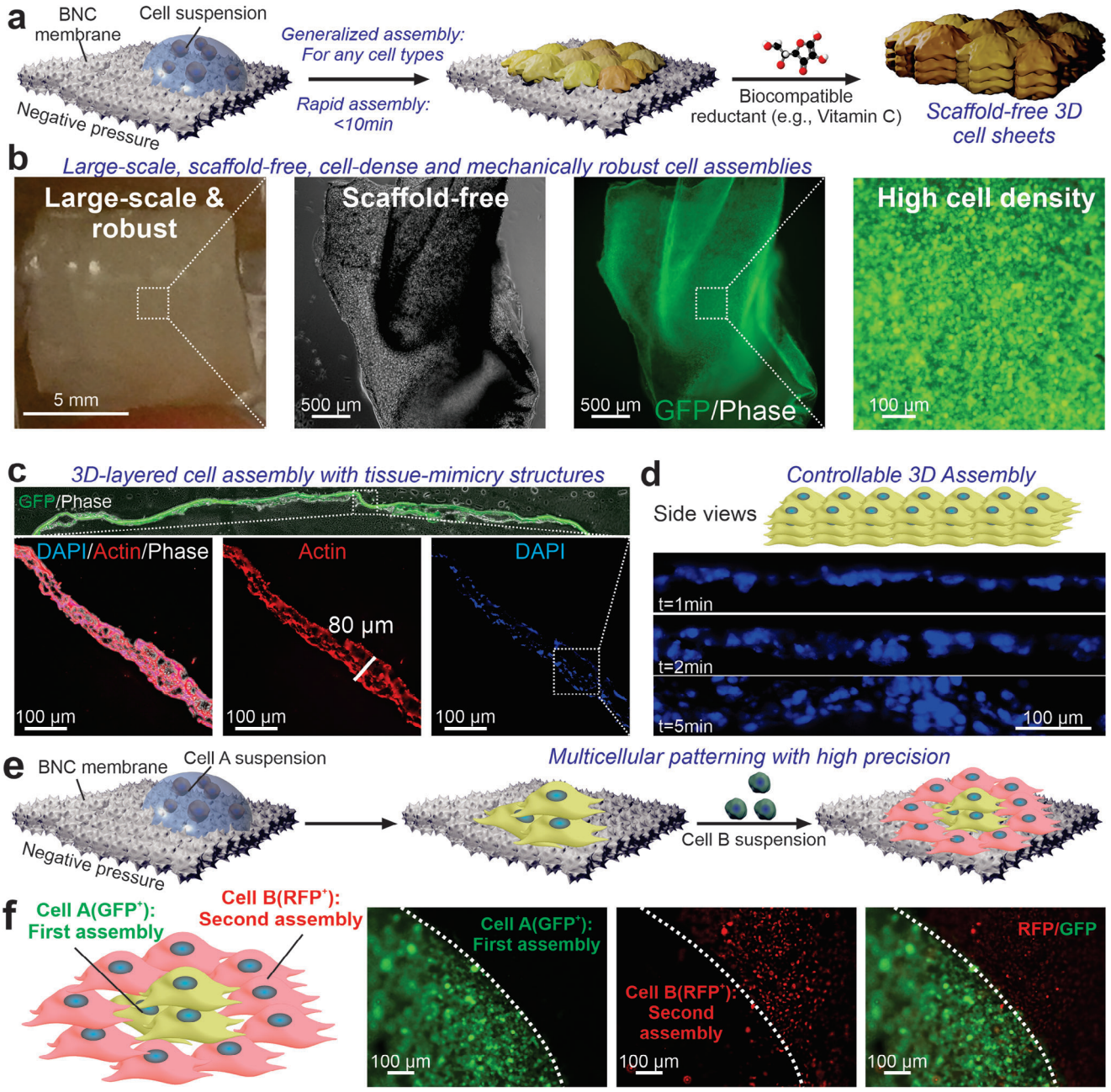

Figure 3. Formation of patterned cell sheets using BNC membrane. a) Schematic diagram illustrating our strategy of cell assembly and formation of scaffold-free 3D cell sheets using BNC membrane-based approaches. After forming the first cell pattern using a PDMS mold with a defined shape, the second layer of cells (Cell B) will be patterned surrounding the first cell type (Cell A). b) Photographs on the left and bright field image in the middle show the stretchable and robust scaffold-free cell sheet assembled from ADMSCs. Fluorescent images showing zoomed-out and zoomed-in images of cell sheets on the right two panels. c) Immunostaining images showing the controllable assembly of ADMSCs into scaffold-free 3D cell sheets. d) Nucleus (DAPI, colored in blue) staining of the cross-sections of 3D ADMSC sheets supporting the controllable assembly of cells on the BNC membrane. e,f) A schematic diagram (e) and fluorescent images (f) showing the sequential assembly of two fluorescently labeled cell lines (Cell A: U87-EGFP cell; Cell B: U87-ERFP cell) into a multicellular pattern in a high precision, which is supported by the minimum mixture of the two cells in the pattern.

negative pressure-guided microparticle assembly method, we were inspired to explore the possibility of integrating a series of controlled negative pressure fields into our BNC membrane-based platform to achieve rapid, controllable, and retrievable cell assembly.[23] Using a negative pressure field to guide the flow of cell suspensions placed on the surface of the membrane, followed by the in situ trapping and stacking of cells into 2D/3D structures, we hypothesized that a rapid and controlled cell assembly could be realized. As the cells in suspension can be quickly aggregated under the negative pressure field, the formation of cell–cell and cell–matrix interactions is faster compared to conventional methods.[3a] To confirm occurrences of these processes, we

performed time-dependent imaging on GFP-labeled cells to more effectively track the cell assembly process. After 5 min of assembly, cell assemblies on the BNC membrane formed a cell sheet with 100% confluency compared to the Matrigel-coated plates, which had confluency ≈80% (Figure 3a,b; Figures S3–S6, Supporting Information). At this stage, we started to observe tissue-level cell densities (>4 × 10^6 cells cm^{-2}) that cannot be achieved in 2D cell cultures even after a prolonged (24 h) seeding process. Increasing cell density is a critical objective in stem cell transplantation, as it optimizes the transplantation process by improving both the efficiency of cell transplantation and the overall integrity of the tissues, particularly where scaffold-free tissues are involved.[24]

We conducted an in-depth analysis of cross-sections on the cellular assemblies on the BNC membrane to demonstrate how our assembly method generates organized 3D tissue structures from diverse cell types. From this study, we observed a distinct 3D-layered tissue structure (3D-cell sheet) in the cross-section fluorescent image (Figure 3c,d). Moreover, the number of cell layers was found to be highly controllable by varying the time and strength of the applied negative pressure field. There was a significant enhancement in cell–cell interactions observed in the 3D-BNC membrane relative to the 2D-BNC membrane that led to an increase in the relative gene expression levels of TGF-β and reduction of apoptotic genes (e.g., Caspase 3) as well as inflammatory genes (e.g., IL6 and TNF) when in co-culture with macrophages (Figure S7, Supporting Information), as checked by gene analysis of a cell–cell signaling biomarker using quantitative real-time polymerase chain reaction (qRT-PCR).

Previously, other 3D cell assembly techniques (e.g., spheroid-based 3D bioprinting) have also been developed, but their application has been restricted to specific cell types with high cell–cell interactions.[25] We hypothesized that our BNC membrane-based cell assembly could address this challenge and be more broadly applicable to different cell types, as the initial cell aggregation does not rely on specific biological interactions. To validate our hypothesis, we systematically tested our cell assembly technique across a comprehensive spectrum of cell types. This included representatives from all three primary germ layers (endoderm, mesoderm, and ectoderm), encompassing stem cells, differentiated somatic cells, and cancer cells. This diverse array of cell types allowed us to rigorously assess the versatility and broad applicability of our approach. Of particular interest was our inclusion of non-adherent cells, such as monocytes, known for their weak cell–cell interactions (**Figure** 4b). The ability to form multilayered cell sheets is interesting as the first layer of cells could block the liquid flow and prevent the deposition of further layers. We speculate that the cells in the suspension are not flat but spherical, so there was still space for assembling additional layers when the initial layer assembled. However, the detailed dynamics of the assembly process would require further investigation. Also, to check if the high cell density in the ADMSC 3D cell sheets would influence cell growth and survival, we analyzed the formed cell sheets in terms of cell number and proliferation-related genes (Figure S7, Supporting Information). From the result (Figure S5, Supporting Information), we could observe fewer total cell counts in ADMSC 3D sheets compared to the low-density 2D monolayer culture after 3 days of culture. This could be attributed to either less cell proliferation or more cell apoptosis. By utilizing our BNC membrane-based techniques, we could showcase the rapid and widespread formation of cells, ultimately forming highly compacted 3D cell sheets.

Most importantly, the BNC membrane-based approach we developed enables precise and versatile cell assembly in three dimensions while offering a fast method to generate robust and scaffold-free tissues. Specifically, the 3D cell sheets assembled on the BNC membrane can be readily retrieved by degrading the BNC membrane under biocompatible conditions. This can be accomplished by incubating the cell-assembled BNC membrane in media containing Vitamin C. We demonstrated the concentration of vitamin C used is harmless to cells over a prolonged (24 h) period (Figure S4, Supporting Information). Even though there have been previous attempts to harvest scaffold-free 2D cell sheets from enzymatically digestible substrates (e.g., collagen), our BNC membrane, with its unique composition and optimized 3D nanochannel structure, demonstrates one of the fastest degradation rates under biocompatible conditions.[26] In this way, a high-density 3D cell assembly is formed from varying cell types, which provides distinct benefits over prior methods. A notable characteristic of our scaffold-free 3D cell sheets is their exceptional robustness during manipulation with surgical tools. This durability, crucial for potential clinical applications, is attributed to the high-density, 3D tissue structures formed by our assembly technique. The ability to withstand handling without compromising structural integrity represents a significant advantage over more fragile conventional cell constructs. That being said, our BNC membrane-based cell assembly method represents a significant advancement in creating and developing versatile, scaffold-free cell sheets. This innovative approach has the potential to revolutionize tissue engineering applications by enabling the fabrication of complex, multicellular structures without the limitations associated with traditional scaffolds. The technique's unique capabilities in generating robust, high-density cellular constructs open up new avenues for developing more physiologically relevant tissue models and improving the efficacy of cell-based therapies.

2.3. Multicellular Patterning on BNC Membranes

Natural tissues are composed of multiple cell types of organized patterns. Therefore, we further showed the formation of multicellular tissue patterns using the BNC membrane-based cell assembly method. To visualize the cell patterning process, two cell lines labeled with GFP (Cell A) and red fluorescence protein (RFP, Cell B) were used for visualization (Figure 3e,f; Figure S7, Supporting Information). We first generated a circular pattern by adding the Cell A suspension onto a polydimethylsiloxane (PDMS) hole mask placed onto the BNC membrane. In this way, the negative pressure field and fluid flow could be confined within the PDMS mask, forming a Cell A pattern onto the membrane. At this stage, the fluid flow was completely blocked due to the presence of the Cell A pattern. So we removed the vacuum and aspirated the media containing Cell A in suspension. To assemble the Cell B layer, we hypothesized that by increasing the negative pressure field that covers the Cell A pattern, the Cell B suspension placed on top of the membrane can be flowed around the Cell A pattern, thereby forming a patterned

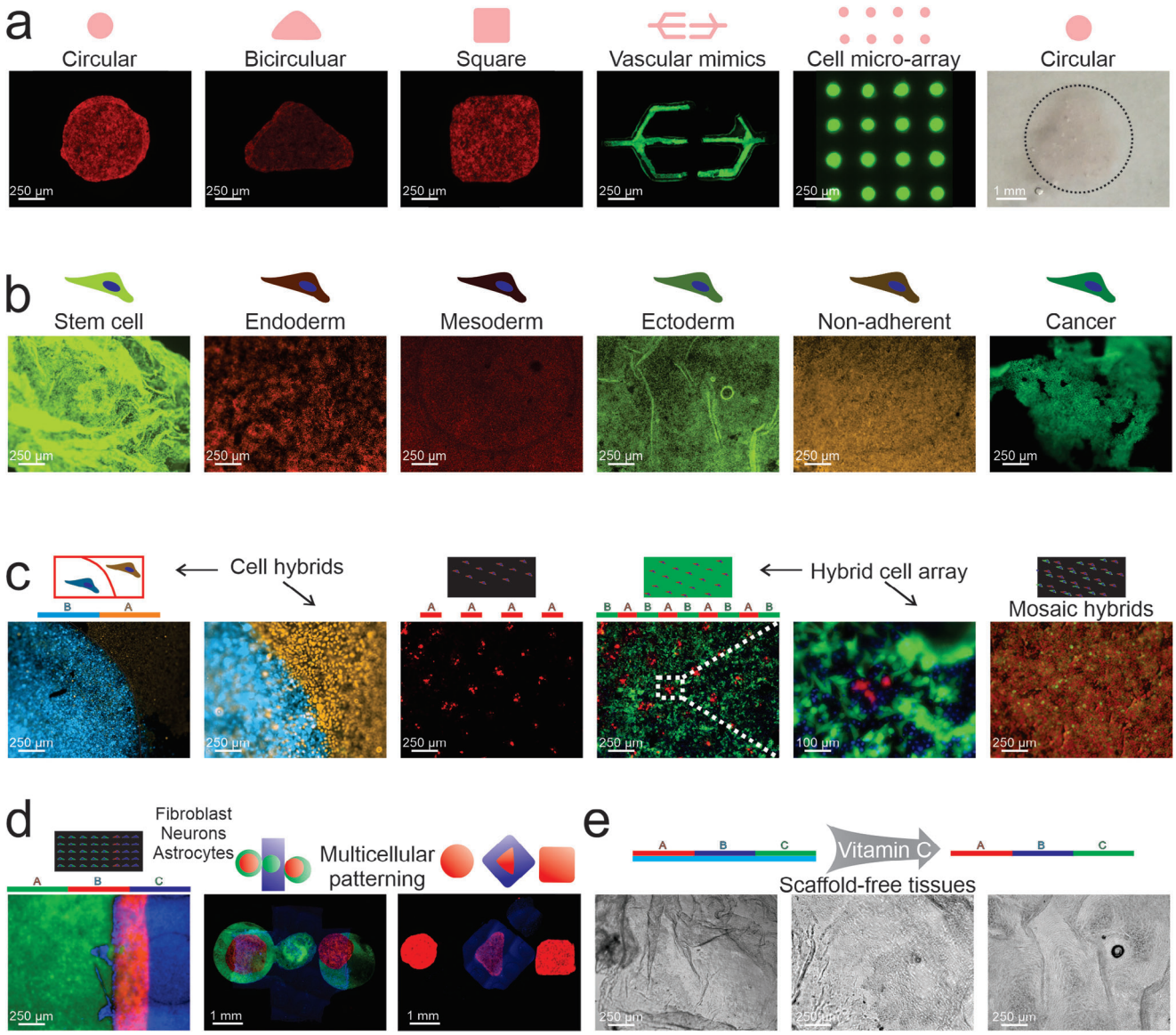

Figure 4. A library of multicellular patterns generated by the BNC-based cell assembly method. a) Schematic diagram illustrating spatially precise deposition of the first and second cell types. A similar approach that uses previously deposited cells as vacuum flow masks can also be extended to more than two cell types. b) 3D cell sheets assembled from distinctively different cell types. c) The spatially controlled assembly of two-cell hybrid tissues and more advanced multi-cellular tissues has been challenging based on conventional approaches. From left to right, core–shell two-cell type hybrid (pseudocolor, blue: U87-ERFP cell; yellow: U87-EGFP cell), cell array hybrid (red: U87-ERFP cell; green: U87-EGFP cell), a mosaic mixture of the U87-ERFP and U87-EGFP cell. d) Fluorescent images showing the multicellular patterns assembled from three or more cell types. The detailed assembly process and cell type description can be found in Figure S4 (Supporting Information). e) Brightfield images of scaffold-free cell sheets after removal of the underlying substrates. The detailed descriptions of each cell type used to form cell patterns can be found in the supporting information.

"core–shell" co-assembly of Cell A and B. We validated our hypothesis using the fluorescence microscope, where we observed a densely packed cell sheet-like structure with Cell A surrounded by Cell B. The high precision of the patterning process was also confirmed by less than 4% mixture of the two colors across the borderline in the two-cell tissue pattern. While a circular shape of the scaffold was used as a proof-of-concept due to its common presence in tissue injuries, our multicellular patterning approach on the BNC membrane can be applied to a variety of biomimicry geometries, including spheroid mimicry dot arrays and blood vessel mimicry stripe patterns (Figure 4a,b). Also, more than two cell types can be assembled to mimic tissues with higher complexities (Figure 4c,d). For instance, we created a macrophage-fibroblast-neuron tri-cellular pattern representative of the scarring spinal cord tissues. Overall, through our development of the BNC membrane-based technique, we have showcased the ability to quickly and precisely assemble cells into both single and multicellular tissues. Most importantly, these tissues can be obtained without relying on scaffolds after cleavage of the BNC membrane (Figure 4d). This advancement allows us to address and surpass

some of the primary limitations present in contemporary tissue engineering practices, laying the groundwork for a wide range of future biomedical applications.

2.4. Skin Inflammation Model for Screening Stem Cell-Derived Therapeutics

To showcase the application of the BNC membrane-based cell sheet assembly approach in modeling chronic inflammation, we further designed and fabricated multicellular patterns composed of macrophages and fibroblasts. Our primary goal was to recapitulate a crucial inflammatory stage in the process of human skin wound healing, as depicted in (**Figure 5a**). It is important to note that human skin wound healing encompasses four distinct stages: homeostasis, inflammation, proliferation, and remodeling.[12] One of the most impeded stages in diabetic chronic wound healing is the inflammation stage, which involves the migration of fibroblasts into the wounded area with high densities of inflammatory cells (e.g., macrophages). Although this process has been studied using in vivo models, there are few demonstrations in creating highly relevant human cell co-culture models to recreate the skin wound tissue structures.[27] Macrophage infiltration plays a dominant role during the inflammatory stage of wound healing. Though macrophages release inflammatory cytokines and influence both fibroblasts and keratinocytes, prior literature has focused more on the outcome of fibroblasts.[15] Therefore, fibroblasts were chosen as a proof-of-concept for the creation of an inflammatory wound healing model. We created this model through patterning of human monocyte-derived macrophages (labeled with Dii dye, colored in red) and human fibroblasts (labeled by CellTracker, colored in green) (Figure 5b). Macrophages were allocated to the center of the pattern, acting as a barrier during the migration of fibroblasts. The BNC membrane is positioned under the cell sheet then removed and subsequently, placed on a bio-inert cellulose membrane to prevent the tissue from folding. As a control, a scratch assay commonly used in industrial evaluation of wound care products was performed using the same fibroblast cell line. In slow-healing skin wounds, the healing rates are generally below 1.0 mm week^{-1}, which is not well represented by the conventional scratch assay (typical healing rates > 1.0 mm day^{-1}), partially due to a lack of proper cellular and molecular barriers during the migration of fibroblasts in those assays.[28] We hypothesized that our macrophage-fibroblast co-culture model could better recapitulate the cellular environments during the migration of fibroblasts and model the natural skin wound healing process. We verified this by investigating the time-dependent migration of fibroblasts across the border of the tissue pattern and observed a much slower migration rate of fibroblasts compared to conventional scratch assays (≈1 mm day^{-1}) (Figure 5b,c; Figure S8, Supporting Information). Although further investigations on the mechanisms of impeded migration in our model are needed, our results indicate the vital role of recreating biomimicry multicellular patterns for skin wound modeling applications.

This improved wound-healing model was then applied to evaluate stem cell-derived therapeutics, which have been clinically tested for treating slow-healing skin wounds. Recent reports suggest that outcomes of stem cell therapies depend highly on cell donors.[29] Thus, having the ability to identify the most efficient donor cells with optimal therapeutic effects can be crucial for treating tissue injuries and skin wounds.[30] As such, we harvested ADMSCs from two different patients (denoted as LAP and 612, respectively) and tested the effects of conditioned media derived from the two donor ADMSCs on the migration of fibroblasts using our co-culture wound-model (Figure 5d,e). We hypothesized that stem cells from different origins would secret different levels of trophic factors for stimulating the migration of fibroblasts and suppressing the inflammation of macrophages, thereby leading to differential outcomes of healing in the wound model. Based on the higher migration rates of fibroblasts observed, we have confirmed that the treatment of conditioned media from the 612 donor cells has a positive effect. In comparison, the control (no treatment) and LAP donor cell-treated groups showed much slower migration rates (Figure 5f–h). Thus, we successfully showed the creation of biomimicry multicellular patterns for modeling skin wounds, further enabling the screening of stem cell-derived therapeutics.

2.5. Accelerated Diabetic Wound Healing using 3D Stem Cell Sheets

Next, we demonstrated enhanced stem cell transplantation for treating diabetic wounds using the BNC membrane. Untimely treatment of diabetic wounds is known to result in detrimental effects such as severe infections that would require amputation of wound areas.[31] Stem cells, once successfully transplanted, can sustainably secret trophic factors for modulating cell migration (e.g., bFGF), inflammation (e.g., IL10), and stimulating vascular formation (e.g., VEGF), thereby holding great potential for treating diabetic wounds (**Figure 6a,b**; Figure S9, Supporting Information). Although 2D stem cell sheets have been tested for diabetic wound treatment with accelerated wound closure, we speculated that the 3D stem cell sheets, assembled from optimal donor cells and created using our BNC membrane-based approach, could more robustly secrete the trophic factors for accelerating diabetic wound healing.[32] This is not only because of the higher cell densities in 3D stem cell sheets, but also supported by recent reports on higher expression of anti-inflammatory and vascularization factors in 3D culture systems.[33] Next, we created a murine diabetic (Type I) skin wound via streptozotocin (STZ) injection, and directly confirmed the significantly accelerated wound closure in the animal group treated by the 3D stem cell sheet (Figure 6c,d). Moreover, histological analysis on the 3D stem cell sheet-treated condition verified enhanced vascularization (blood vessel branches), reduced inflammation (immunostaining on the CD11b macrophage marker), and higher proliferation (immunostaining on the PH3 proliferation marker), thereby strongly supporting our hypothesis (Figure 6d,e; Figure S10 and S11, Supporting Information). Furthermore, the transplanted 3D stem cell sheet (cells visualized by green fluorescence from the CellTracker dye staining) was found to be highly robust, with their tissue structure preserved 1-week after the transplantation and strongly adhering to the wound sites without requiring any suture or glue. Thus, we have successfully demonstrated the capabilities of the BNC membrane-based technique for

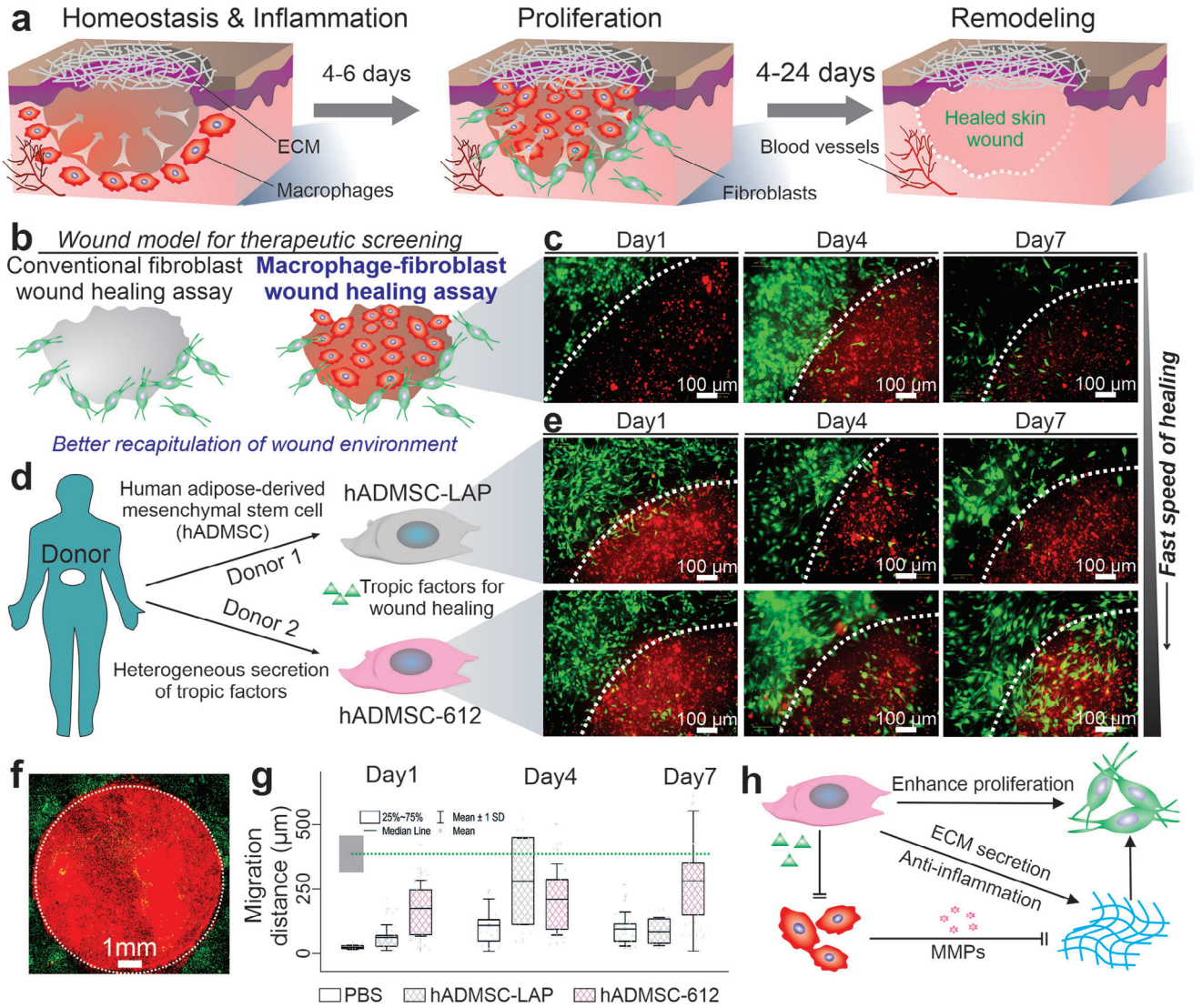

Figure 5. Biomimetic skin inflammation models for screening stem cell-based therapeutics. a,b) Schematic diagram showing the major stages of human wound healing. One of the critical steps in the inflammation stage is the skin cell migration into the wound area in the presence of macrophages. However, current models (e.g., scratch assay has been mostly based on a single type of skin cell such as fibroblasts) have not recapitulated this process well. c) BNC membrane-based generation of the desired fibroblast-macrophage pattern to mimic the multi-cellular skin wound structures and investigation of time-dependent skin cell migration (wound closure) in this fibroblast-macrophage pattern. To visualize the two different cell patterns, GFP-labelled fibroblasts were used and THP-1 monocyte-derived macrophages were labelled in red using DiL dye. d,e) This skin wound model was used to evaluate and predict the therapeutic outcomes of the treatment of human adipose-derived mesenchymal stem cells (hADMSCs) derived from different donors. The conditioned media from specific stem cell cultures was added into the skin wound model culture as a treatment. The time-dependent migration of the fibroblast was monitored for both stem cell condition media-treated conditions and was compared to the control condition (normal cell culture media). f) A large-area fluorescent image showing the fibroblast-macrophage pattern that mimics the shape of skin wounds. g) Quantification of the time-dependent wound closure using different stem cell-based treatments in the skin wound model based on fibroblast-macrophage patterns. h) Explanations on the differences of fibroblast migration after treatment by condition media from stem cells derived from different donors. Stem cells from different donors may have different capabilities of secreting trophic factors in promoting cell proliferation, migration, and anti-inflammation, resulting in different therapeutic outcomes.

fabricating 3D stem cell sheets. Furthermore, our novel method has significantly improved the effectiveness of stem cell therapy, particularly in treating chronic wounds that have historically had slow healing rates. To comprehensively validate the wound healing efficacy of our cell sheets in the diabetic mouse model, it is essential to expand our analysis to include additional key biomarkers. Specifically, future studies should examine markers associated with vascularization (e.g., CD31, VEGF), re-epithelialization (e.g., cytokeratin, E-cadherin), and extracellular matrix remodeling (e.g., collagen types I and III, fibronectin). These investigations will provide a more nuanced understanding of the cell sheets' multifaceted role in promoting tissue regeneration and could reveal potential mechanisms underlying their therapeutic effects in diabetic wound healing.[31]

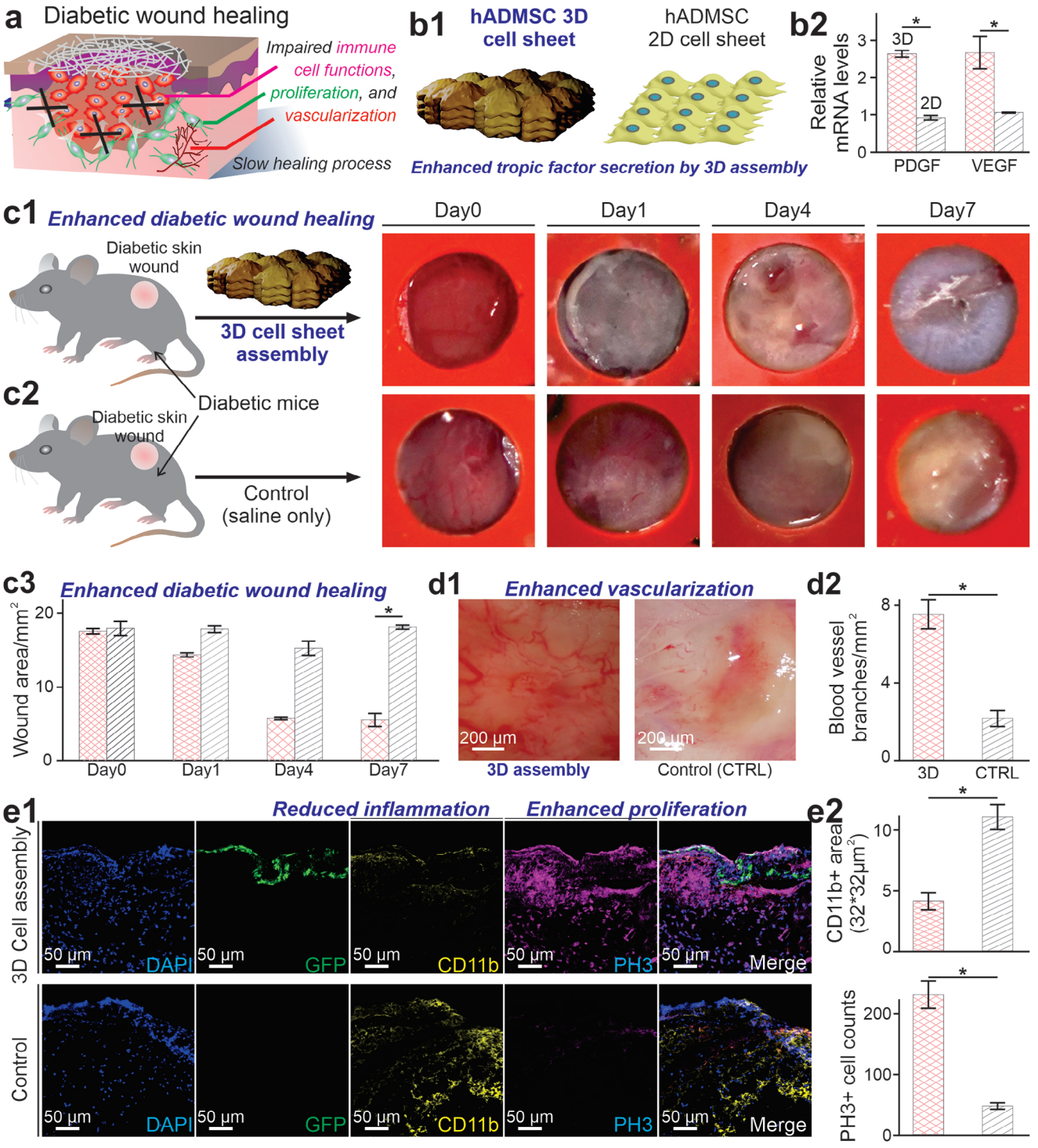

Figure 6. Accelerated Diabetic Wound Healing using 3D Stem Cell Sheets. a) A schematic diagram illustrating the mechanisms of the slow healing rate of diabetic wounds, including impaired immune cell functions, reduced proliferation rates, and limited vascularization capacity due to high glucose levels. b) We aim to address these challenges in diabetic wound healing by transplanting the scaffold-free 3D hADMSC sheets, which show higher expression of cytokines that may facilitate the angiogenesis and proliferation of skin cells. c) Time-dependent wound closure in control animals with diabetic wounds (c1) and 3D hADMSC sheet-treated murine diabetic wounds (c2). Our results confirm the significantly accelerated wound closure rates by treating 3D hADMSC sheets formed by the BNC membrane-based method. d,e) Enhanced vascularization (photographs shown in d1, summary graph shown in d2), reduced inflammation, and enhanced proliferation (immunostaining images shown in e1, summary graphs shown in e2) from the transplantation of our 3D hADMSC sheet to the murine diabetic wounds. $n = 3$, $^*p < 0.05$ by student's t-test.

3. Discussion

Controlled and programmable 3D cell assembly has broad clinical applications in tissue repair and disease modeling but is currently challenging.[34] To this end, we demonstrated an innovative approach that utilizes BNC membranes to create 3D scaffold-free tissues and cell assemblies. The BNC membrane-based cell assembly method was then demonstrated for producing scaffold-free 3D tissues with high cell densities. Using the BNC membrane-based cell assembly, we can precisely and reliably control the 3D structures of tissues. This method allows for bio-inspired, heterogeneous cell patterning across various cell types. By implementing this BNC membrane-based assembly technique, we could craft an advanced model for wound healing. Furthermore, we utilized this model to assess the therapeutic efficacy of stem cells derived from human donors. Our studies demonstrate that transplantation of 3D scaffold-free tissues, generated using the BNC membrane-based cell assembly method, significantly accelerates injury repair. This enhanced therapeutic efficacy has been consistently observed in both in vitro models and in vivo experiments, providing robust evidence for the potential clinical application of this approach. The ability to reliably achieve accelerated tissue regeneration underscores the advantages of our method in creating functional, transplantable tissue constructs for regenerative medicine. Given the immense potential of scaffold-free tissue engineering and cell patterning, this innovative assembly technique is well-positioned to become a fundamental platform in the field, enabling the development of advanced tissue models and therapeutic applications. The ability to accurately and efficiently manipulate cell assembly opens up unprecedented opportunities for progress in tissue engineering, potentially revolutionizing approaches to complex medical challenges and laying the groundwork for future innovations in healthcare.

Moving forward, while Vitamin C-supplemented media does not significantly influence cell viability, further studies should be performed to confirm its impact on stem cell transcriptome. Furthermore, it is crucial to demonstrate that the BNC membrane-based cell assembly can produce 3D structured tissues, constructing cell structures with over ten layers either by stacking or in combination with 3D bioprinting techniques. Moreover, current tissue engineering technologies primarily focus on recreating tissue assemblies with high cell densities, such as epithelial layers, the central nervous system, liver, and muscle. However, the human body also contains cell-sparse tissues, including cartilage and bone, which present unique challenges for tissue engineering and require further development of appropriate technique. Therefore, it is crucial to realize the limitations of current technology in their applications in both treating and modeling tissue diseases with minimal cell–cell interactions. In the future, it would also be essential to examine the detailed histological improvement of BNC membrane-based approach as compared to conventional wound healing strategies, including the PNIPAM polymer-based cell sheet technology, single cell injection, and hydrogel-based transplantation of stem cells. Although the current study demonstrates a proof-of-concept application in modeling and treating wound healing, the overall outcome is still in its early stages. Thoroughly verifying the advantages of this approach over current tissue engineering methods requires additional studies. Moreover, fully understanding its potential for clinical translation is also crucial. By addressing the current constraints associated with cell structures, the BNC membrane-based cell assembly would hold excellent potential for unique clinical applications that demand the creation of intricate tissue structures.

Supporting Information

Supporting Information is available from the Wiley Online Library or from the author.

Acknowledgements

K.-B.L. acknowledges the partial financial support from the NSF (CBET-1803517), the New Jersey Commission on Spinal Cord (CSCR17IRG010; CSCR16ERG019), NIH R21 (R21AR071101), and NIH R01 (1R01DC016612, 1R01NS130836-01A1, 3R01DC016612-01S1, and 5R01DC016612-02S1), NIH RM1 (RM1 NS133003-01), NIH R21 (R21 NS132556-01), Alzheimer's Association (AARG-NTF-21-847862), CDMRP (OCRP, OC220235P1), NJ Commission on Cancer Research (COCR23PPR007), and HealthAdvance (NHLBI, U01HL150852). L.Y. acknowledges the financial support from the National Natural Science Foundation of China (Grant No. 32301106) and the Fundamental Research Funds for the Central Universities (22120240435). The authors acknowledge Brandon M. Conklin and Shavin Patel for their generous help on nanomaterial synthesis.

Conflict of Interest

The authors declare no conflict of interest.

Data Availability Statement

The data that support the findings of this study are available from the corresponding author upon reasonable request.

Keywords

biodegradable nanochannel membrane, cell assembly, cell sheet engineering, multicellular constructs, stem cell therapy, tissue engineering, wound healing

Received: February 25, 2024
Revised: July 7, 2024
Published online: July 24, 2024

[1] a) A. J. Stevens, A. R. Harris, J. Gerdts, K. H. Kim, C. Trentesaux, J. T. Ramirez, W. L. McKeithan, F. Fattahi, O. D. Klein, D. A. Fletcher, W. A. Lim, *Nature* **2023**, *614*, 144; b) G. R. Chao, T. M. Wannier, C. Gutierrez, N. C. Borders, E. Appleton, A. Chadha, T. Lebar, G. M. Church, *Cell* **2022**, *185*, 3551.
[2] C. Trentesaux, T. Yamada, O. D. Klein, W. A. Lim, *Cell Stem Cell* **2023**, *30*, 10.
[3] a) V. M. Gaspar, P. Lavrador, J. Borges, M. B. Oliveira, J. F. Mano, *Adv. Mater.* **2020**, *32*, 1903975; b) S. A. Yi, Y. Zhang, C. Rathnam, T. Pongkulapa, K.-B. Lee, *Adv. Mater.* **2021**, *33*, 2007949.

[4] a) Y. Haraguchi, T. Shimizu, T. Sasagawa, H. Sekine, K. Sakaguchi, T. Kikuchi, W. Sekine, S. Sekiya, M. Yamato, M. Umezu, T. Okano, *Nat. Protoc.* **2012**, *7*, 850; b) N. Matsuda, T. Shimizu, M. Yamato, T. Okano, *Adv. Mater.* **2007**, *19*, 3089; c) A. Shahin-Shamsabadi, J. Cappuccitti, *Adv. Funct. Mater.* **2024**, *34*, 2308552.
[5] C. J. Bashor, I. B. Hilton, H. Bandukwala, D. M. Smith, O. Veiseh, *Nat. Rev. Drug DiscoveryDiscov.* **2022**, *21*, 655.
[6] a) K. I. Ritzau-Reid, S. J. Callens, R. Xie, M. Cihova, D. Reumann, C. L. Grigsby, L. Prados-Martin, R. Wang, A. C. Moore, J. P. Armstrong, *Adv. Mater.* **2023**, *35*, 2300305; b) K. Sadtler, A. Singh, M. T. Wolf, X. Wang, D. M. Pardoll, J. H. Elisseeff, *Nat. Rev. Mater.* **2016**, *1*, 16040; c) J. Lou, D. J. Mooney, *Nat. Rev. Chem.* **2022**, *6*, 726; d) C. A. DeForest, B. D. Polizzotti, K. S. Anseth, *Nat. Mater.* **2009**, *8*, 659.
[7] a) S. V. Murphy, A. Atala, *Nat. Biotechnol.* **2014**, *32*, 773; b) J. G. Roth, L. G. Brunel, M. S. Huang, Y. Liu, B. Cai, S. Sinha, F. Yang, S. P. Pașca, S. Shin, S. C. Heilshorn, *Nat. Commun.* **2023**, *14*, 4346.
[8] a) B. Ayan, D. N. Heo, Z. Zhang, M. Dey, A. Povilianskas, C. Drapaca, I. T. Ozbolat, *Sci. Adv.* **2020**, *6*, eaaw5111; b) J. Zhang, Y. Xu, C. Zhuo, R. Shi, H. Wang, Z. Hu, H. F. Chan, H.-W. Kim, Y. Tao, M. Li, *Biomaterials* **2023**, *294*, 122014; c) M. Hao, W. Wang, A. Kumar, W. H. A. Kamaruddin, S. Saidin, N. A. N. N. Malek, J. Claverie, H. Liu, *BMEMat* **2023**, *2*, e12059.
[9] a) J. Wang, H. Qiao, Z. Wang, W. Zhao, T. Chen, B. Li, L. Zhu, S. Chen, L. Gu, Y. Wu, Z. Zhang, L. Bi, P. Chen, *Adv. Mater.* **2023**, *35*, 2210631; b) Y. Zhu, X. Zhang, L. Sun, Y. Wang, Y. Zhao, *Adv. Mater.* **2023**, *35*, 2210083. c) B. Gong, X. Zhang, A. A. Zahrani, W. Gao, G. Ma, L. Zhang, J. Xue, *Exploration* **2022**, *2*, 20210035.
[10] M. E. Todhunter, N. Y. Jee, A. J. Hughes, M. C. Coyle, A. Cerchiari, J. Farlow, J. C. Garbe, M. A. LaBarge, T. A. Desai, Z. J. Gartner, *Nat. Methods* **2015**, *12*, 975.
[11] a) J. Almeida-Pinto, M. R. Lagarto, P. Lavrador, J. F. Mano, V. M. Gaspar, *Adv. Sci.* **2023**, *10*, 2304040; b) Y. Hu, Y. Duan, K. Salaita, *Angew. Chem., Int. Ed.* **2023**, *62*, 202302967.
[12] V. Falanga, *Lancet* **2005**, *366*, 1736.
[13] V. Falanga, R. R. Isseroff, A. M. Soulika, M. Romanelli, D. Margolis, S. Kapp, M. Granick, K. Harding, *Nat. Rev. Dis. Primers* **2022**, *8*, 50.
[14] a) Q. Li, C. Wang, X. Li, J. Zhang, Z. Zhang, K. Yang, J. Ouyang, S. Zha, L. Sha, J. Ge, *J Tissue EngEng.* **2023**, *14*, 20417314231168529; b) X. Ye, E. Zhang, Y. Huang, F. Tian, J. Xue, *Wound Repair Regener.* **2023**, *32*, 195; c) A. Ko, C. Liao, *BMEMat* **2023**, *1*, e12037.
[15] Z. Li, Y. Zhao, H. Huang, C. Zhang, H. Liu, Z. Wang, M. Yi, N. Xie, Y. Shen, X. Ren, J. Wang, J. Wang, *Adv. Healthcare Mater.* **2022**, *11*, 2201524.
[16] S. Li, J. Wang, Y. Lv, Z. Cui, L. Wang, *Adv. Funct. Mater.* **2023**, *34*, 2308176.
[17] a) M. Liu, M. Yang, X. Wan, Z. Tang, L. Jiang, S. Wang, *Adv. Mater.* **2023**, *35*, 2208995; b) J. Ding, J. Zhang, J. Li, D. Li, C. Xiao, H. Xiao, H. Yang, X. Zhuang, X. Chen, *Prog. Polym. Sci.* **2019**, *90*, 1.
[18] S. Zhang, L. Shen, H. Deng, Q. Liu, X. You, J. Yuan, Z. Jiang, S. Zhang, *Adv. Mater.* **2022**, *34*, 2108457.
[19] J. L. Young, X. Hua, H. Somsel, F. Reichart, H. Kessler, J. P. Spatz, *Nano Lett.* **2020**, *20*, 1183.
[20] a) R. Yang, Y. Fan, R. Ye, Y. Tang, X. Cao, Z. Yin, Z. Zeng, *Adv. Mater.* **2021**, *33*, 2004862; b) C. Rathnam, L. Yang, S. Castro-Pedrido, J. Luo, L. Cai, K.-B. Lee, *Sci. Adv.* *7*, eabj2281; c) C. Rathnam, L. Yang, S. Castro-Pedrido, J. Luo, L. Cai, K.-B. Lee, *Sci. Adv.* **2021**, *7*, eabj2281.
[21] a) G. Eda, G. Fanchini, M. Chhowalla, *Nat. Nanotechnol.* **2008**, *3*, 270; b) X. Zhang, H. Cheng, H. Zhang, *Adv. Mater.* **2017**, *29*, 1701704.
[22] K. Xing, J. Ge, W.-X. Wang, X. Geng, X.-P. Shen, J.-L. Tang, L.-B. Qu, Y.-Q. Sun, Z.-H. Li, *New J. Chem.* **2019**, *43*, 9466.
[23] J. J. Kim, K. W. Bong, E. Reátegui, D. Irimia, P. S. Doyle, *Nat. Mater.* **2017**, *16*, 139.
[24] N. Vapniarsky, L. W. Huwe, B. Arzi, M. K. Houghton, M. E. Wong, J. W. Wilson, D. C. Hatcher, J. C. Hu, K. A. Athanasiou, *Sci. Transl. Med.* **2018**, *10*, eaaq1802.
[25] C. F. Guimarães, A. P. Marques, R. L. Reis, *Adv. Mater.* **2022**, *34*, 2105645.
[26] J. Kobayashi, A. Kikuchi, T. Aoyagi, T. Okano, *J. Biomed. Mater. Res., Part A* **2019**, *107*, 955.
[27] D. S. Masson-Meyers, T. A. Andrade, G. F. Caetano, F. R. Guimaraes, M. N. Leite, S. N. Leite, M. A. C. Frade, *Int. J. Exp. Pathol.* **2020**, *101*, 21.
[28] B. Dalisson, J. Barralet, *Adv. Healthcare Mater.* **2019**, *8*, 1900764.
[29] a) P. Cahan, G. Q. Daley, *Nat. Rev. Mol. Cell Biol.* **2013**, *14*, 357; b) D. G. Phinney, *J. Cell. Biochem.* **2012**, *113*, 2806.
[30] T. Wang, J. Zhang, J. Liao, F. Zhang, G. Zhou, *Stem Cells Transl. Med.* **2020**, *9*, 1495.
[31] O. A. Peña, P. Martin, *Nat. Rev. Mol. Cell Biol.* **2024**, *25*, 599.
[32] a) Y. Kato, T. Iwata, S. Morikawa, M. Yamato, T. Okano, Y. Uchigata, *Diabetes* **2015**, *64*, 2723; b) J. Yu, M.-Y. Wang, H.-C. Tai, N.-C. Cheng, *Acta Biomater.* **2018**, *77*, 191.
[33] a) K. Carter, H. J. Lee, K.-S. Na, G. M. Fernandes-Cunha, I. J. Blanco, A. Djalilian, D. Myung, *Acta Biomater.* **2018**, *99*, 247; b) S. Abd El-Aleem, E. Jude, *J. Cytol. Histol.* **2018**, *9*, 1000519; c) J. Mao, L. Chen, Z. Cai, S. Qian, Z. Liu, B. Zhao, Y. Zhang, X. Sun, W. Cui, *Adv. Funct. Mater.* **2022**, *32*, 2111003.
[34] A. Ovsianikov, A. Khademhosseini, V. Mironov, *Trends Biotechnol.* **2018**, *36*, 348.